



# Turbulence characteristics in the tropical mesosphere as obtained by MST radar at Gadanki (13.5° N, 79.2° E)

M. N. Sasi, L. Vijayan

## ► To cite this version:

M. N. Sasi, L. Vijayan. Turbulence characteristics in the tropical mesosphere as obtained by MST radar at Gadanki (13.5° N, 79.2° E). *Annales Geophysicae*, 2001, 19 (8), pp.1019-1025. hal-00316895

HAL Id: hal-00316895

<https://hal.science/hal-00316895>

Submitted on 18 Jun 2008

**HAL** is a multi-disciplinary open access archive for the deposit and dissemination of scientific research documents, whether they are published or not. The documents may come from teaching and research institutions in France or abroad, or from public or private research centers.

L'archive ouverte pluridisciplinaire **HAL**, est destinée au dépôt et à la diffusion de documents scientifiques de niveau recherche, publiés ou non, émanant des établissements d'enseignement et de recherche français ou étrangers, des laboratoires publics ou privés.

# Turbulence characteristics in the tropical mesosphere as obtained by MST radar at Gadanki ( $13.5^{\circ}$ N, $79.2^{\circ}$ E)

M. N. Sasi and L. Vijayan

Space Physics Laboratory, Vikram Sarabhai Space Centre, Trivandrum 695022, India

Received: 7 November 2000 – Revised: 16 May 2001 – Accepted: 13 June 2001

**Abstract.** Turbulent kinetic energy dissipation rates ( $\varepsilon$ ) and eddy diffusion coefficients ( $K_z$ ) in the tropical mesosphere over Gadanki ( $13.5^{\circ}$  N,  $79.2^{\circ}$  E), estimated from Doppler widths of MST radar echoes (vertical beam), observed over a 3-year period, show a seasonal variation with a dominant summer maximum. The observed seasonal variation of  $\varepsilon$  and  $K_z$  in the mesosphere is only partially consistent with that of gravity wave activity inferred from mesospheric winds and temperatures measured by rockets for a period of 9 years at Trivandrum ( $8.5^{\circ}$  N,  $77^{\circ}$  E) (which shows two equinox and one summer maxima) lying close to Gadanki. The summer maximum of mesospheric  $\varepsilon$  and  $K_z$  values appears to be related to the enhanced gravity wave activity over the low-latitude Indian subcontinent during the southwest monsoon period (June – September). Both  $\varepsilon$  and  $K_z$  in the mesosphere over Gadanki show an increase with an increase in height during all seasons. The absolute values of observed  $\varepsilon$  and  $K_z$  in the mesosphere (above  $\sim 80$  km) does not show significant differences from those reported for high latitudes. Comparison of observed  $K_z$  values during the winter above Gadanki with those over Arecibo ( $18.5^{\circ}$  N,  $66^{\circ}$  W) shows that they are not significantly different from each other above the  $\sim 80$  km altitude.

**Key words.** Meteorology and atmospheric dynamics (middle atmosphere dynamics; tropical meteorology; wave and tides)

## 1 Introduction

Gravity waves play an important role in the dynamical coupling between the lower and the middle atmosphere. These gravity waves are essentially generated in the troposphere by various mechanisms, such as topography (e.g. Nastrom et al., 1987; Nastrom and Fritts, 1992), convective and frontal activity (e.g. Clark et al., 1986; Fritts and Nastrom, 1992), wind shear (e.g. Fritts, 1982, 1984) and jet stream (e.g. Fritts

and Luo, 1992). As these waves propagate upwards their amplitudes increase with an increase in height due to a decrease in atmospheric density. At higher levels, especially at mesospheric heights, the wave amplitude becomes so large that instability sets in, leading to wave breaking, turbulence generation and wave saturation (e.g. Hodges, 1967, 1969). The instability can either be convective or dynamic. Turbulence can be generated by processes such as non-linear breaking and critical level interactions of these waves. Apart from limiting the growth of the wave, the turbulence transports energy and momentum extracted from the wave, contributing to the eddy diffusion process in the mesosphere.

Turbulence in the mesosphere plays a very significant role in the energy budget and thermal structure. It may heat the atmosphere by dissipation of the turbulent energy and turbulent eddies will transport heat to different atmospheric regions. These eddies will also transport momentum and constituents affecting the circulation and vertical distribution of minor constituents, respectively. Both in-situ measurements of neutral and plasma density fluctuations by rocket payloads (e.g. Lubken et al., 1987; 1993; Blix et al., 1990) and remote radar measurements (Gage and Balsley, 1984; Hocking 1985; 1990) of turbulence intensities are used by different researchers to investigate turbulence parameters in the mesosphere-lower thermosphere (MLT) region. In the in-situ measurements, turbulence parameters are derived by fitting a theoretical model to the measured spectrum of the density fluctuations. In the radar method, both the received signal power and the broadening of the Doppler spectrum are utilized to deduce the turbulence parameters in the MLT region (Hocking, 1989). Though the radar method of obtaining the turbulence parameters is less accurate when compared to the in-situ method, the radar technique allows for nearly continuous measurements and may be used to study the seasonal variability of turbulence at different locations all over the globe.

In this paper, turbulence parameters deduced from the Indian mesosphere – stratosphere – troposphere (MST) radar observations in the MLT region over Gadanki ( $13.5^{\circ}$  N,  $79.2^{\circ}$

Correspondence to: M. N. Sasi (mnsasi@md4.vsnl.net.in)

E) are presented. The method of extracting the turbulence parameters from the VHF radar observations is briefly presented in Sect. 2. Section 3 deals with the results obtained from the radar data. These results are compared with those obtained by other researchers. A summary and conclusions are given in Sect. 4.

## 2 Data and method of analysis

The data used in this study of the turbulence parameters in the MLT region were obtained by the Indian MST radar located at Gadanki ( $13.5^{\circ}$  N,  $79.2^{\circ}$  E). This radar is a high-power VHF phased array radar operating at  $\sim 53$  MHz in coherent backscatter mode with an average power aperture product of  $7 \times 10^8$  W m<sup>2</sup>. Transmitted power is 2.5 MW (peak) and fed to the  $32 \times 32$  Yagi antenna array generating a radiation pattern with a gain of 36 dB and one-way beam width of  $\sim 3^{\circ}$ . The radar beam can be positioned in any zenith angle. For the present set of observations, both  $10^{\circ}$  and  $20^{\circ}$  oblique beams were used. More detailed specifications of the radar system are given in Rao et al. (1995). The data used in this study are collected from the MST radar operating at Gadanki for different seasons (spread over a total of 10 calendar months) in 1994, 1995 and 1996 using a five beam configuration of the radar with a height resolution of 1.2 km during the daytime (1000–1500 hrs). The radar was operated for 3–5 days a month (except for the months of February and May) during these years.

Hocking (1989) basically describes two methods to derive turbulence parameters from the radar data: one from the backscattered power received by the radar and the other from the Doppler spectral width measurements. The use of the first method requires the calibration of the radar to estimate the received power, whereas for the second method, such a procedure is not necessary. In this paper, turbulence parameters in the MLT region are estimated using the second method, namely, the Doppler spectral width technique. In using the spectral width method to deduce the turbulence parameters, one has to follow the detailed procedures as outlined by Hocking (1989). The first step is to remove all the echoes, which occur due to specular reflections. In the classical picture of turbulent echoes, echo power varies linearly with spectral width. It is reasonable to select turbulent echoes based on this criterion. However, a close examination of this procedure revealed that all specular reflection echoes were not removed by this procedure alone. Additionally, echoes which have very narrow spectral widths and very large peaks were also filtered out to remove the remaining specular reflection echoes. By adopting this procedure, most of the specular reflection echoes (possibly a few turbulent echoes as well) were removed. Then for these selected echoes, a correction to the Doppler broadening due to non-turbulent processes has to be performed. Two major factors contributing to the Doppler spectral width are the finite width of the beam and the vertical shear of the total horizontal winds. Time variation of vertical and horizontal winds due to the presence

of gravity waves can also contribute to the broadening of the Doppler spectrum depending on the time duration used for forming the Doppler spectra. In our observations, this time duration is primarily  $\sim 20$  seconds and the broadening due to buoyancy waves may be neglected. Essentially, one determines the spectral broadening due to these non-turbulent processes and subtracts it from the experimentally observed spectral width in order to arrive at the spectral broadening due to the turbulence alone and hence, the mean square velocity of turbulent fluctuations ( $\bar{v}^2$ ) in the MLT region. From the  $\bar{v}^2$  profile, one can estimate the turbulent kinetic energy dissipation rate ( $\varepsilon$ ) and the turbulent eddy diffusion coefficient ( $K_z$ ).

Although, in principle, both vertical and oblique beams can be used for the estimate of  $\varepsilon$ , small-scale horizontal fluctuations which can arise on scales of less than one pulse-length, can also contribute to  $\bar{v}^2$ . Hence, a vertical beam may, preferably, be used for the estimation of  $\varepsilon$ . Nevertheless, if oblique beams are used in conjunction with a vertical beam, it is possible to extract not only estimates of  $\varepsilon$ , but also estimates of the magnitudes of the horizontal fluctuating motions associated with gravity waves with periods of the order of the data integration times, and with gravity waves with the vertical wavelength less than about one pulse length (Hocking, 1985). In our analysis only vertical beams will be used to obtain turbulent parameters in the MLT region.

Total observed spectral width is given by (e.g. Czechowsky and Ruster, 1997)

$$\sigma_{\text{observed}}^2 = \sigma_{\text{turb}}^2 + \sigma_{\text{beam}}^2 + \sigma_{\text{shear}}^2 \quad (1)$$

It is seen that two major factors contributing to the observed spectral width due to non-turbulent processes are the finite width of the radar beam and the vertical shear of the total horizontal wind. Thus, one has to determine the spectral broadening due to a non-turbulent process and subtract it from the experimentally observed spectral width in order to arrive at the spectral broadening due to turbulence alone.

In our study,  $\sigma_{\text{shear}}$  can be neglected in the case of vertical echoes and hence, the mean square velocity fluctuations can be written as

$$\bar{v}^2 = \sigma_{\text{turb}}^2 = \sigma_{\text{observed}}^2 - \sigma_{\text{beam}}^2 \quad (2)$$

where

$$\sigma_{\text{beam}}^2 = V^2 \frac{\theta_{1/2}^2}{2.76} \quad (3)$$

where  $V$  is the total horizontal wind and  $\theta_{1/2}$  is the half power, half-width of the main radar beam.  $\sigma_{\text{turb}}$  is the root mean square fluctuating velocity ( $\bar{v}$ ) due to turbulence within the illuminated volume. It may be mentioned that  $\sigma_{\text{observed}}$  and  $\sigma_{\text{beam}}$  used in Eq. (2) are half-power half-widths, and  $\sigma_{\text{turb}}^2$  obtained from (2) has to be converted to sigma-width by multiplying by a factor of .72 for obtaining  $\bar{v}$  (Fukao et al., 1994).

The kinetic energy dissipation rate  $\varepsilon$ , as given by Hocking (1989), can be calculated as

$$\varepsilon = 3.1 \bar{v}^2 f_B \quad (4)$$

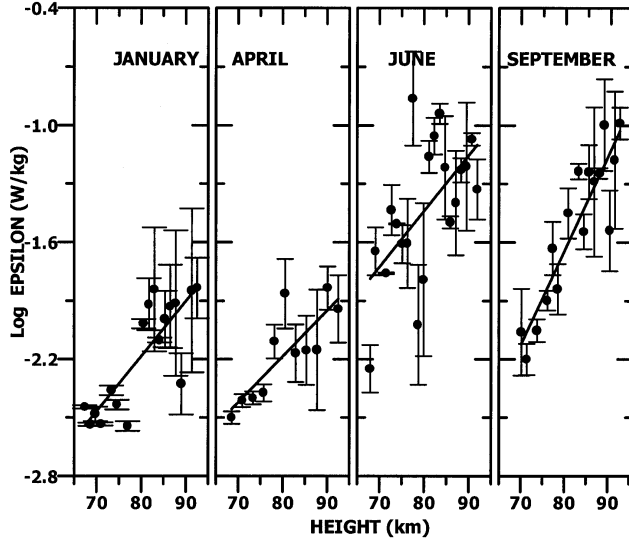


**Fig. 1.** Height variations of the kinetic energy dissipation rates ( $\epsilon$ ) in the mesosphere for the months of January, April, June and September over Gadanki. Vertical bars show standard errors in  $\epsilon$  values. The best-fit line for the height variation of  $\epsilon$  is shown by a straight line.

And the vertical eddy diffusion coefficient, as given by Weinstock (1978), is

$$K_z = C(\epsilon/\omega_B^2) \quad (5)$$

where  $\omega_B$  is the BV frequency and given by

$$\omega_B = 2\pi f_B \quad (6)$$

and  $C = 0.81$ .  $\omega_B$  is calculated from the climatological temperature profile given for the  $8.5^\circ \text{N}$  latitude (Sasi and Sengupta, 1986) in the  $60\text{--}80 \text{ km}$  region and from the CIRA 1986 model for the  $80\text{--}100 \text{ km}$  region.

Hocking (1989) briefly mentions the uncertainties in the value of the constant  $C$  in Eq. (5). McIntyre (1989) discusses in detail the uncertainties of the value of  $C$  in terms of the supersaturation of the gravity waves responsible for the generation of turbulence. His thought experiment shows that the value of  $C$  is varying in a way that depends sensitively on the value of the wave supersaturation, and the use of  $C$  values of order unity could lead to gross errors in the computed values of  $K_z$ . In addition to the uncertainties in the value of the constant  $C$ , uncertainties in the value of the Brunt-Vaisala frequency appearing in Eq. (5) can also lead to uncertainties in the derived value of the eddy diffusion coefficient. Ideally, the Brunt-Vaisala frequency in the turbulent layer is the one to use. But we are only using climatological values, which can differ greatly from the actual values prevalent in the turbulent layer at the time of observation. This argument is equally applicable to the computation of  $\epsilon$  as well.

$\sigma_{\text{observed}}$  is the observed spectral width of the Doppler spectrum and is obtained directly from the second moment of the Doppler spectra. The mean square velocity fluctuation

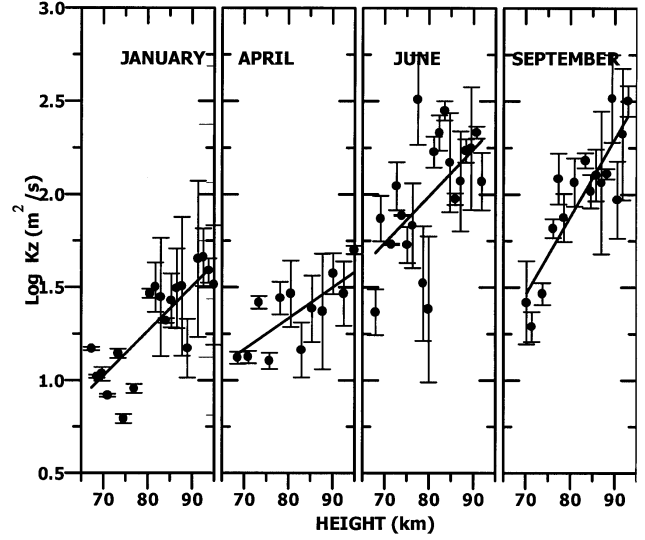


**Fig. 2.** Same as Fig. 1, but for vertical eddy diffusion coefficient ( $K_z$ ).

is obtained from  $\sigma_{\text{turb}}^2$ , as mentioned earlier. The total horizontal winds,  $V$ , are derived from the oblique beam data. In using Eqs. (4) and (5), one has to bear in mind an important assumption involved in arriving at those equations. It is assumed that the term  $\sigma_{\text{turb}}^2$  is consisting entirely of the mean square velocity fluctuations within the volume illuminated by the radar pulse, and that these fluctuations are contributed equally by inertial range turbulence and buoyancy range turbulence (Hocking, 1989). However, any departure from this assumption will cause an uncertainty in  $\epsilon$  if the fractional contribution of inertial range turbulence is different from 0.5.

### 3 Results and discussion

Figure 1 shows the height variations of the turbulent kinetic energy dissipation rate  $\epsilon$  for the months of January, April, June and September, representing winter, vernal equinox, summer and autumn equinox, respectively. The standard errors in  $\epsilon$ , computed from the averaging of all values derived from all echoes at a height during all the days in a month, are shown as vertical bars in the figure. A linear best-fit is made to the height variation of  $\epsilon$  and is shown in Fig. 1. In general, it is found that  $\epsilon$  values are in the range of  $\sim 3\text{--}75 \text{ mW kg}^{-1}$  during the months of January and April, and  $\sim 7\text{--}100 \text{ mW kg}^{-1}$  during the months of June and September. It is observed that  $\epsilon$  generally increases with an increase in height and reaches maximum around the  $90\text{--}95 \text{ km}$  height region during all four months. The general tendency of increasing  $\epsilon$  with increase in height is observed during other months as well. Apparently during the period from June to September  $\epsilon$  values remain high throughout the  $\sim 65\text{--}95 \text{ km}$  height region when compared to those values during other months.

Figure 2 shows similar height profiles for the eddy diffusion coefficient  $K_z$ . Standard errors in  $K_z$  are also computed

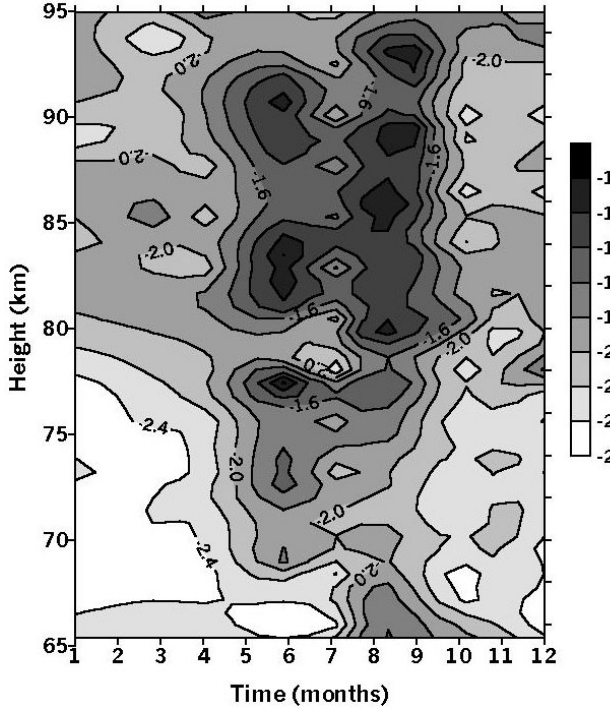


**Fig. 3.** Height-time section of energy dissipation rates ( $\varepsilon$ ) in the mesosphere over Gadanki. The contour intervals are  $.2 \text{ W/kg}$  (log scale).

and shown as error bars in the figure. Similar to the variation of  $\varepsilon$  with height,  $K_z$  also generally increases with increase in height during the four months of January, April, June and September, as shown in Fig. 2. During the months of January and April,  $K_z$  values lie in the range of  $\sim 10 - 40 \text{ m}^2 \text{ s}^{-1}$  in the  $65 - 95 \text{ km}$  height region, with the larger values occurring at greater heights. The corresponding  $K_z$  values during June and September vary in the range of  $\sim 25 - 300 \text{ m}^2 \text{ s}^{-1}$ . In the case of  $K_z$ , maximum values are also observed, occurring during the period from June to September.

The height-time cross section of the turbulent energy dissipation rate  $\varepsilon$  is shown in Fig. 3. It is observed that the turbulence intensity is as a maximum during the June to September period with lower values occurring during other times. It may be mentioned that the broad maximum in  $\varepsilon$  values occurs during the June to September period, which is the southwest monsoon period over the Indian subcontinent. Similar features are observed for the seasonal variation of  $K_z$  as well (not shown).

If the observed enhancement of  $\varepsilon$  and  $K_z$  during the June to September period is associated with the gravity wave activity, then one may expect a corresponding enhancement in gravity wave activity as well. In order to see any seasonal variation of mesospheric gravity wave activity, M-100 rocket data from 1978 to 1986 at Trivandrum ( $8.5^\circ \text{ N}$ ,  $77^\circ \text{ E}$ ), located close to Gadanki, were examined. M-100 rockets measured winds and temperatures in the  $25 - 80 \text{ km}$  region once a week. The amplitudes of upward propagating gravity waves

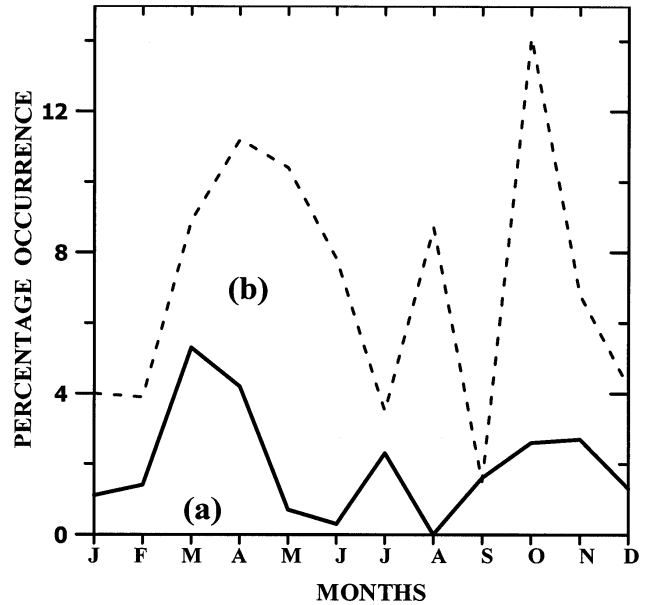


**Fig. 4.** Seasonal variations of proxies for gravity wave activity in the mesosphere (M-100 rocket data) – See text. (a) Percentage occurrence of temperature lapse rates  $> 6 \text{ K km}^{-1}$  in the mesosphere ( $65 - 80 \text{ km}$ ) over Trivandrum ( $8.5^\circ \text{ N}$ ,  $77^\circ \text{ E}$ ) for a period of 9 years (solid curve), (b) Same as (a) but for Richardson number  $< 1$  (dashed curve).

attain large values at mesospheric heights due to the exponential decrease in atmospheric density with an increase in height, and are eventually limited by instabilities and lead to wave breaking, as well as generation of turbulence and wave saturation (e.g. Lindzen, 1981). The instability can be either convective when the wave plus the background state have a negative stability or dynamic when the Richardson number ( $Ri$ ) has a value less than 0.25. Ideally, one will be able to compute these two parameters from mesospheric temperatures and winds, which are measures of instabilities. But the temperature and wind profiles are smoothed (in height), due to limitations in the processing procedures of M-100 rocket data, so that a portion of the vertical variation is essentially removed from the profiles. The smoothing of M-100 rocket data results in very significant attenuation of vertical variation in temperatures and winds with scales less than  $\sim 5 \text{ km}$ . In spite of this smoothing, wind and temperature values are given at every km height interval. However, a tendency for the occurrence of instabilities can be computed from these profiles.

Using the M-100 rocket data we have estimated the frequency of occurrence of temperature lapse rates ( $-dT/dz$ ;  $T$  is the temperature and  $z$  is the height) greater than  $6 \text{ K km}^{-1}$  (proxy for convective instabilities), and  $Ri$  less than 1 (proxy for shear instability) for every month during 1978–1986 in the  $65 - 80 \text{ km}$  height region. The frequency of occurrence is expressed as a percentage of the total number of observed lapse rates and  $Ri$ , respectively. This frequency is plotted in Fig. 4 for every month. The actual frequency of occurrence

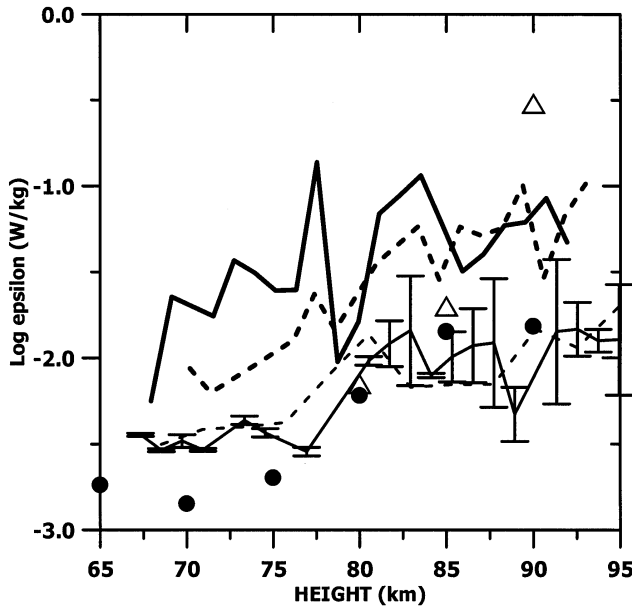


**Fig. 5.** A comparison of the energy dissipation rates ( $\varepsilon$ ) in the mesosphere over Gadanki with those obtained by others. Thin solid, thin dashed, thick solid and thick dashed lines represent  $\varepsilon$  over Gadanki for the months of January, April, June and September, respectively. Solid circles and triangles represent  $\varepsilon$  values reported by Lubken et al. (1993) and Hocking (1990), respectively. Vertical bars show standard errors in  $\varepsilon$  values over Gadanki in January.

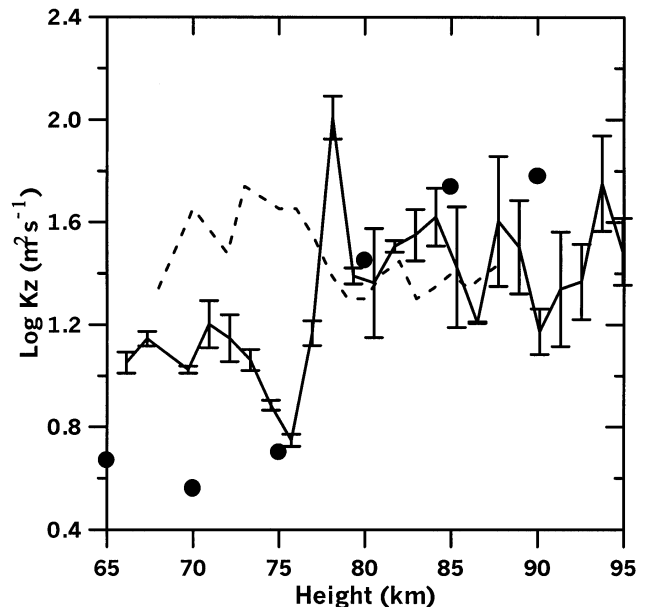


**Fig. 6.** A comparison of the eddy diffusion coefficients ( $K_z$ ) in the mesosphere over Gadanki with those obtained by others. Solid line represents  $K_z$  over Gadanki for the month of December. Dashed line and solid circles represent winter values of  $K_z$  obtained by Röttger (1986) over Arecibo (18.3° N, 66° W) and Lubken et al. (1993) over high latitudes, respectively. Vertical bars show standard errors in  $K_z$  values over Gadanki in December.

of these two parameters may be much higher than that shown in this figure because of the inherent smoothing of the M-100 data. Both the parameters show minimum during the winter solstice and maxima during the equinoxes. There exists one secondary maximum during summertime for both the parameters (large lapse rates during July and small  $R_i$  during August). However, it may be noted that secondary maximum during summertime is comparable to the maxima during the equinoxes. If these parameters can be considered as indirect measures of the occurrence of instabilities in the mesosphere, which are presumably the result of very large amplitudes of gravity waves, then their seasonal variation may imply a similar variation in the gravity wave activity. An earlier study by Hirota (1984) using rocket data had indicated similar semianual maxima around the equinoxes for gravity wave activity in the equatorial middle atmospheric region.

The seasonal variation of  $\varepsilon$  displayed in Fig. 1 and Fig. 3 shows a broad maximum during the months of June to September, whereas that of  $-dT/dz$  and  $R_i$ , displayed in Fig. 4, shows two equinox maxima and one summer maximum. Recent observational studies which make use of balloon-measured temperature data show that gravity wave potential energy ( $E_p$ ) in the stratosphere at low latitudes ( $10^{\circ}$  S– $20^{\circ}$  S) has a clear annual variation with a maximum during the monsoon months (rainy season) of December to February (Allen and Vincent, 1995). Using temperature profiles obtained by the GPS/MET experimental data, Tsuda et al. (2000) show that in the 20–30 km height region,  $E_p$  is

maximizing during the southern hemispheric summer in the low-latitude regions, such as Indonesian archipelago. Similarly, a recent study using a Microwave Limb Sounder (MLS) onboard the Upper Atmosphere Research Satellite (UARS) by McLandress et al. (2000) shows that during the northern hemispheric summer (June to August), gravity wave activity at the  $\sim 38$  km level has a maximum lying on and near the Indian subcontinent. McLandress et al. also show that wave activity maxima are correlated with, to a large degree, the satellite measurements of outgoing longwave radiation, indicating that deep convection is the source of these waves. These studies mentioned above show that stratospheric gravity wave activity in low latitudes is maximizing during the wet season, implying tropical convection as the source of these waves. Can this strong seasonal variation in the stratospheric gravity wave activity produce a similar seasonal variation in the mesosphere? Apparently the summer peak shown in Fig. 4 may correspond to this situation in the mesosphere and one may expect enhanced gravity wave activity in the mesosphere during summer. It is, therefore, possible that the enhancement of the observed turbulent energy dissipation rate and the vertical eddy diffusion coefficient in the mesosphere over Gadanki is related to the enhanced gravity wave activity over the low latitude Indian subcontinent during the summer monsoon season (June to September).

It will be interesting to see whether any similar relationship between gravity wave activity and turbulence exists at other latitudes as well. A good correspondence between

the gravity wave activity and eddy diffusivity due to turbulence observed by MU radar in the mesosphere over Shigaraki, Japan ( $35^{\circ}$  N,  $136^{\circ}$  E) is reported in the literature. The observational study by Tsuda et al. (1990) shows that mesospheric gravity wave activity has a semiannual variation with solstice maxima, and Kurosaki et al. (1996) show a very similar seasonal variation for the eddy diffusivity in the mesosphere over Shigaraki with maxima during the solstice periods. These two observations support the hypothesis that turbulence is primarily generated by gravity wave breaking in the mid-latitude mesospheric region. A similar mechanism may be operating in the low-latitude mesosphere also, but with a summer (wet season) maximum in gravity wave activity and turbulence parameters.

A comparison has been made between the  $\varepsilon$  values obtained from the present study and the values observed at other geographical locations (Lubken et al., 1993; Hocking, 1990). It is found that  $\varepsilon$  values over Gadanki during January and April are very close to those at other latitudes, especially at greater heights (Fig. 5). But during the summer season,  $\varepsilon$  values over Gadanki are much larger when compared to those at higher latitudes below the 80 km height. Yet above 80 km the differences are not significant. Fig. 6 shows a comparison of  $K_z$  values over Gadanki with those of Lubken et al. (1993) for a high latitude winter and those of Röttger (1986) for a low latitude winter over Arecibo ( $18.3^{\circ}$  N,  $66^{\circ}$  W). The values over Gadanki are shown for the month of December. It is seen that below about the 75 km height, the  $K_z$  values are smaller (not very significantly) when compared to those over Arecibo. Above the  $\sim 80$  km height, there is hardly any difference between the two sets of  $K_z$  values. Below  $\sim 75$  km,  $K_z$  values over Gadanki are larger when compared to those from Lubken et al. (1993). Above the  $\sim 75$  km height the differences between the two are not significant.

#### 4 Summary and conclusions

A method following Hocking (1989) is used to calculate the turbulence parameters from MST radar data in the MLT region. It is found that the turbulence parameters, estimated over Gadanki, show maximum values during the Indian summer monsoon (June to September). The turbulence parameters generally show an increase with an increase in height during all seasons. An examination of the seasonal variation of gravity wave activity in the nearby location Trivandrum shows that gravity wave activity proxies estimated from rocket-measured wind and temperature data have a seasonal variation with equinox and summer maxima. However, recent studies of gravity waves using balloon and satellite data show that stratospheric gravity wave activity over low-latitudes maximizes during the wet season in both northern and southern hemispheres. This seasonal variation of gravity wave activity may cause a similar variation in the mesosphere and may be responsible for the observed summer maxima of mesospheric  $\varepsilon$  and  $K_z$  values over Gadanki, resulting from the gravity wave breakdown leading to enhanced turbulence

generation during the period. The turbulence parameters estimated over Gadanki show that above 80 km, their values are not significantly different from those reported for high latitudes by in-situ measurements and other low-latitude radar measurements.

**Acknowledgements.** The National MST Radar Facility (NMRF) is operated as an autonomous facility under DOS with partial support from CSIR. The authors are very thankful to the scientists and engineers from NMRF for making the MST radar observation a success. Authors gratefully acknowledge many helpful and constructive comments by the referees, which helped in the improvement of the manuscript.

Topical Editor J.-P. Duvel thanks two referees for their help in evaluating this paper.

#### References

- Allen, S. J., and Vincent, R. A., Gravity wave activity in the lower atmosphere: Seasonal and latitudinal variations, *J. Geophys. Res.*, 100, 1327–1350, 1995.
- Blix, T. A., Thrane, E. V., Fritts, D. C., von Zahn, U., Lubken, F.-J., Hillert, W., Blood, S. P., Mitchell, J. D., Kokin G. A., and Pakhamov, S. V., Small-scale structure observed in-situ during MAC/EPSILON, *J. Atmos. Terr. Phys.*, 52, 835–854, 1990.
- Czechowsky, P. and Ruster, R., VHF radar observations of turbulent structures in the polar mesopause region, *Ann. Geophysicae*, 15, 1028–1036, 1997.
- CIRA 1986, COSPAR international reference atmosphere: 1986, Part II: Middle atmosphere models, edited by D. Rees, J. J. Barnett, and K. Labitzke, pp. 357–381, Pergamon Press, Elmsford, New York, 1990.
- Clark, T. E., Hauf, T., and Kuettner, J. P., Convectively forced internal gravity waves: Results from two-dimensional numerical experiments, *Quart. J. Roy. Meteorol. Soc.*, 112, 899–925, 1986.
- Fritts, D. C., Shear excitation of atmospheric gravity waves, *J. Atmos. Sci.*, 39, 1936–1952, 1982.
- Fritts, D. C., Shear excitation of atmospheric gravity waves, part II: Non-linear radiation from a free shear layer, *J. Atmos. Sci.*, 41, 524–537, 1984.
- Fritts, D. C. and Luo, Z., Gravity wave excitation by geostrophic adjustment of the jet stream, Part I: Two-dimensional forcing, *J. Atmos. Sci.*, 49, 681–697, 1992.
- Fritts, D. C. and Nastrom, G. D., Sources of mesoscale variability of gravity waves II: Frontal, convective, and jet stream excitation, *J. Atmos. Sci.*, 49, 111–127, 1992.
- Fukao, S., Yamanaka, M. D., Ao, N., Hocking, W. K., Sato, T., Yamamoto, M., Nakamura, T., Tsuda, T., and Kato, S., Seasonal variability of vertical eddy diffusivity in the middle atmosphere. 1. Three-year observations by the middle and upper atmosphere radar, *J. Geophys. Res.*, 99, 18973–18987, 1994.
- Gage, K. S. and Balsley, B. B., MST radar studies of wind and turbulence in the middle atmosphere, *J. Atmos. Terr. Phys.*, 46, 739–753, 1984.
- Hirota, I., Climatology of gravity waves in the middle atmosphere, in Dynamics of the Middle Atmosphere, edited by J. R. Holton, and T. Matsuno, Terra Scientific Publishing Company, Tokyo, Japan, 65–67, 1984.
- Hocking, W. K., Measurement of turbulent energy dissipation rates in the middle atmosphere by radar techniques: a review., *Radio Sci.*, 20, 1403–1422, 1985.

- Hocking, W. K., Target parameters estimation, MAP Hand Book, 30, 228–268, 1989.
- Hocking, W. K., Turbulence in the region 80–120 km., *Adv. Space Res.*, 10 (12), 153–161, 1990.
- Hodges, R. R., Generation of turbulence in the upper atmosphere by internal gravity waves, *J. Geophys. Res.*, 72, 3455–3458, 1967.
- Hodges, R. R., Eddy diffusion coefficients due to instabilities in internal gravity waves, *J. Geophys. Res.*, 74, 4087–4090, 1969.
- Kurosaki, S., Yamanaka, M. D., Hashiguchi, H., Sato, T., and Fukao, S., Vertical eddy difusivity in the lower and middle atmosphere: a climatology based on the MU radar observations during 1986–1992, *J. Atmos. Terr. Phys.*, 58, 727–734, 1996.
- Lindzen, R. S., Turbulence and stress owing to gravity waves and tidal breakdown, *J. Geophys. Res.*, 86, 9707–9714, 1981.
- Lubken , F.-J., von Zahn, U., Thrane, E. V., Blix, T., Kokin, G. A., and Pakhomov, S. V., In-situ measurements of turbulent energy dissipation rates and eddy diffussion coefficients during MAP/WINE, *J. Atmos. Terr. Phys.*, 49, 763–775, 1987.
- Lubken, F.-J., Hillert, W., Lehmacher, G., and von Zahn, U., Experiments revealing small impact of turbulence on the energy revealing small impact of turbulence on the energy budget of the mesosphere and lower thermosphere, *J. Geophys. Res.*, 98, 20369–20384, 1993.
- McIntyre, M. E., On dynamics and transport near the polar mesopause in summer, *J. Geophys. Res.*, 94, 14617–14628, 1989.
- McLandress, C., Alexander, M. J., and Wu, D. L., Microwave Limb Sounder observations of gravity waves in the stratosphere: A climatology and interpretation , *J. Geophys. Res.*, 105, 11947–11967, 2000.
- Nastrom, G. D. and Fritts, D. C., Sources of mesoscale variability of gravity waves, I: Topographic excitation, *J. Atmos. Sci.*, 49, 101–110, 1992.
- Nastrom, G. D., Fritts, D. C., and Gage, K. S., An investigation of terrain effects on the mesoscale spectrum of atmospheric motions, *J. Atmos. Sci.*, 44, 3087–3096, 1987.
- Rao, P. B., Jain, A. R., Kishore, P., Balamuralidhar, P., Damle, S. H., and Viswanathan, G., Indian MST radar 1, system description and sample vector wind measurements in ST mode, *Radio Sci.*, 30, 1125–1138, 1995.
- Röttger, J., The use of experimentally deduced Brunt-Vaisala frequency and turbulent velocity fluctuations to estimate the eddy diffusion coefficient, *MAP Handbook*, 20, 173–178, 1986.
- Sasi, M. N. and Sengupta, K. , A reference atmosphere for Indian equatorial zone from surface to 80 km–1985, Scientific report SPL: SR:006:85, Space Physics Laboratory, Vikram Sarabhai Space Centre, Trivandrum, India, 1986.
- Tsuda, T., Murayama, Y., Yamamoto, M., Kato, S., and Fukao, S., Seasonal variations of momentum flux in the mesosphere observed with the MU radar, *Geophys. Res. Lett.*, 17, 725–728, 1990.
- Tsuda, T., Nishida, M., Rocken, C., and Ware, R. H., A global climatology of gravity wave activity in the stratosphere revealed by the GPS occultation data (GPS/MET), *J. Geophys. Res.*, 105, 7257–7273, 2000.
- Weinstock, J., Vertical turbulent diffusion in a stably stratified fluid, *J. Atmos. Sci.*, 35, 1022–1027, 1978.